Indian Journal of Chemistry
Vol. 57A, May 2018, pp. 610-618

Papers

Photoinduced pyrene degradation in contaminated soils by polyaniline coated photocatalysts

F Shahrezaei[a], A Hemati Azandaryani[b], A M Mansourie[c], A Akhbari[d] & P Pakravan[e,] *

[a]Academic Center for Education, Culture & Research (ACECR), Kermanshah, Iran

[b]Nano Drug Delivery Research Center, Kermanshah University of Medical Sciences, Kermanshah, Iran

[c]Research Center for Environmental Determination of Health (RCEDH), Kermanshah University of Medical Sciences, Kermanshah, Iran

[d]Department of Civil Engineering, Faculty of Engineering, University of Malaya, Kuala Lumpur, Malaysia

[e]Department of Chemistry, Zanjan Branch, Islamic Azad University, Zanjan, Iran

Email: pakravanparvaneh@iauz.ac.ir

Received 11 February 2018; revised and accepted 20 April 2018

Polyaniline (PA) coated TiO_2 and ZnO nanoparticles have been used to improve the photocatalytic efficiency of pyrene degradation in soil samples. The interfacial polymerization method is used to prepare the polyaniline coated ZnO and TiO_2 nanocomposites, which are characterized by scanning electron microscopy, Fourier transform infrared spectroscopy, and X-ray diffraction. The SEM images and the SPSS analysis demonstrate the particle size distribution in the range of 100–400 nm. The surface charge of the polyaniline coated TiO_2 and ZnO nanocomposites are found to be 19.5 and 21.2 mV, respectively. The pyrene removal efficiency is more than 95% on the polymer coated photocatalysts surface. The high degradation efficiency of the polyaniline coated ZnO and TiO_2 nanocomposites is probably due to the high capacity of polyaniline for the adsorption of pollutants from the contaminated soils; the semiconducting behavior is reflected in the chain structure of the polymer under both ultraviolet and visible irradiation. Enhanced photocatalytic activity for degradation of pyrene under UV and visible light, is possibly due to the synergistic effect of PA and NPs.

Keywords: Photocatalysts, Photodegradation, Nanocomposites, Pyrene degradation, Soil contamination, Polyaniline, Titanium, Zinc oxide

Polycyclic aromatic hydrocarbons (PAHs) belong to the widely dispersed class of human carcinogens in the environment. PAHs are formed during incomplete combustion of hydrocarbons and fossil fuels[1-3]. PAHs can be adsorbed on solid matrices, which then sediment and collect in fish and other aquatic animals and this hazardous material may enter the human body through seafood consumption. Soil is the environmental sink for PAHs, although they have also been detected in water, air, and vegetation. Pyrene, a four ringed PAH is a cytotoxic agent with low biodegradability and high persistency. Pyrene is considered as a priority pollutant by the United States' Environmental Protection Agency (US EPA) due to its carcinogenic and mutagenic effects[4]. Therefore, there is a need to develop more effective methods for purifying pyrene polluted environments including soil, air, water, and sediments.

In recent years, many strategies, such as solvent extraction, phytoremediation, chemical, and biological methods, have been devised for removing PAH pollutants from contaminated soils and waters[5-7]. These approaches are often very expensive and may produce other pollutants. To overcome these disadvantages, advanced oxidation processes (AOPs) have attracted the attention of researchers. The AOPs are based on the *in situ* generation of hydroxyl radicals ($^{\bullet}OH$), which are capable of destroying an extensive variety of pollutants[8]. The hydroxyl radical ($^{\bullet}OH$) has an oxidation potential of $E°$ = +2.8 V which is much greater than that of some other oxidants (e.g., ozone: 2.07 V, hydrogen peroxide: 1.78 V, hypochlorous acid: 1.49 V)[9]. Among the advanced oxidation processes, heterogeneous photocatalysts such as titanium dioxide (TiO_2) and zinc oxide (ZnO) under ultraviolet (UV) light have attracted the attention of researchers due to their ability to degrade and eliminate hazardous organic pollutants from air, water, and earth, in addition to their low toxigenicity, cost-effectiveness, high chemical stability, and wide band gap energy[10, 11].

The main disadvantage of conventional photocatalysts is their large-band gap which requires

UV light excitation. TiO_2 and ZnO nanoparticles can absorb only UV light, which initiates photodegradation. UV light constitutes less than 5% of solar irradiation which is too low to achieve high photodegradation over a short period of time[6, 12].

Hence, several efforts have been made towards the preparation and characterization of visible-light-active photocatalytic nanoparticles by doping with organic or inorganic materials. This has been reported as a promising strategy for improving the photocatalytic efficiency[13-15].

Most polymers are insulators because the valence electrons are tightly held to their parent atoms and produce relatively few free electrons. When the movement of free electrons is restricted, no current can flow, making them insulators. However, certain classes of polymeric materials exhibit semiconducting behavior. Their electronic properties and band gaps can be tuned by altering the polymer side chains or the chemical nature of the polymer backbone[16]. Polymers such as polythiophene, polyaniline (PA), polypyrrole, polypyrenes, and poly(*p*-phenylene vinylene) have received much attention for use in electronic devices, chemical and biological sensors, and in the design and fabrication of well-organized and cost-effective solar cells. Moreover, they have remarkable physicochemical and electrical properties such as low cost, low operating temperature, flexibility, and easy operation. One of the main usage of semiconductor polymers in the photocatalytic applications is for wastewater treatment[17]

In recent years, studies have been carried out on the photocatalytic oxidation and treatment or removal of pollutants using polyaniline (PA)-based nanomaterials[18, 19]. In this study, we have investigated the effect of PA doping on the TiO_2 and ZnO NPs in the pyrene degradation. The nanocomposites were characterized by scanning electron microscopy (SEM), Fourier transform infrared spectroscopy (FT-IR), and X-ray diffraction (XRD). To reach the optimum degradation efficacy, the effects of PA doping, initial dosing, and the time under both visible and UV light irradiation on the contaminated soils were investigated.

Materials and Methods

Pyrene and aniline were purchased from Sigma-Aldrich. Hydrochloric acid, ammonium persulphate, methanol, high-performance liquid chromatography (HPLC) grade acetonitrile, and acetone were obtained from Merck (Germany). In this work, deionized water was used for the preparation of solutions and for subsequent dilution. The specified pyrene stock solution was prepared by dissolving the pollutant in acetone.

Preparation of PA modified ZnO and TiO_2 nanocomposites

The ZnO-PA, and TiO_2-PA nanocomposites were prepared via *in situ* interfacial polymerization method[20]. Briefly, a fixed amount of distilled aniline (0.05 mole, 4.5 g) with varying amounts of TiO_2 or ZnO (0.045 and 0.09 g respectively) were added to HCl in an ice bath. Then, an aqueous solution of ammonium persulphate (0.04 mole, 9 g) was added dropwise to the medium as an oxidizing agent. The reaction was continued for one hour till completion. The obtained dark green precipitate was filtered, washed with methanol-water mixture (50:50 *v/v*) to remove any unreacted monomer, and then dried at 60-70 °C.

Characterization of the PA coated photocatalyst composites

The particles' size was analyzed by the scanning electron microscopy using a Philips XL30 microscope at 26 kV accelerating voltage. After drying the particles for 12 h, the sample was coated with a platinum layer using an SCDOOS sputter coater (Bal-Tec, Sweden) in an argon atmosphere. The samples were scanned and the photomicrographs were obtained. The size of the nanocomposites was evaluated by the Microstructure Measurement Software (Nahamin pardazon Asia Co.)[21]. The particle size and the standard deviation were calculated by the SPSS analysis.

X-ray diffraction (XRD) patterns of the samples were obtained on a Equnox diffractometer (Inel Co.) operating with a Cu anode. The X-ray tube was sealed at room temperature at 35 kV voltage and 20 mA current. The 2θ scans were recorded using Cu Kα radiation of wavelength 1.548 Å in the range of 20°–80°. The Fourier transform infrared (FTIR) spectroscopy of the NPs was obtained by using an FTIR spectrophotometer (AVATAR 370, Nicolet, USA).

The surface charge (zeta potential) of the nanocomposites was measured using the photon correlation spectroscopy (PCS, Malvern Zetasizer Nano-ZS, Malvern, UK). The NPs were diluted with deionized water and sonicated for several minutes for measuring the zeta potential.

Preparation of pyrene contaminated bentonite and clay samples

The contaminated bentonite and clay soils were prepared by placing 10.0 g of the soils in a glass tube

which was completely closed. The composition of the minerals in both, clay and bentonite soil, by XRF analysis for quantification of soil constituents and XRD for the type of constituents is given in Table S1 (Supplementary Data). A certain amount of pyrene (1 mg for 10.0 g of soils) in acetone solution was added to 10 g of the investigated soil samples and placed in a glass tube that was completely sealed. The resulting contaminated soil samples were mixed with a shaker for four hours. The contaminated soil samples were kept in steady condition in dark for three days for the pyrene to be completely absorbed in the bentonite and clay soil samples. The acetone in the samples, volatilized in vacuum at room temperature, and the contaminated bentonite and clay soil samples were then placed in dark environment for further experiments. The amount of the pyrene in the soils was kept at a level of 100 mg kg^{-1}.

Pyrene degradation in contaminated soil samples by TiO_2-PA and ZnO-PA nanocomposites

The effect of the reaction time (1, 2, 4 h) and nanocomposite dosage (2.5, 3.75, 5.00, 10% (*w/w*) equal to 0.025, 0.0375, 0.05, and 100 mg for 1.0 g of the total weight of the investigated samples) on the pyrene degradation were carried out under exposure to UV radiation. To determine the effect of polyaniline doping on the photocatalytic activity, first the effects of pure TiO_2 and ZnO NPs on pyrene degradation were investigated. While the effect of TiO_2 on the pyrene degradation has been studied under UV-irradiation by Dong and coworker[22], in the present study, further experiments of photocatalytic activity have been done under both the UV and vis radiation and PA doping on the TiO_2 and ZnO NPs. To study the effect of sunlight, 1.0 g of the pyrene-contaminated soils (1.0 g) were taken in an agate mortar to which the required quantity of the prepared nanocomposites was added and mixed. The samples were then removed and placed in a Petri dish and diluted with deionized water. The samples were then placed under natural sunlight (at 10 a.m.) at a suitable temperature varying from 25–30 °C. Under both, the UV and sunlight condition the soil samples were dissolved in acetonitrile by shaking for extracting the remaining pyrene from the soils. The pyrene concentration in the acetonitrile extract was determined by HPLC.

Pyrene extraction from the treated soils

Pyrene was extracted from the soil samples by the continuous batch withdrawal technique. In the batch extraction procedure, the pyrene-containing contaminated soils were mixed with 10 mL of acetonitrile and taken in a 15 mL centrifuge tube, and agitated for 30 min in a shaker. After complete extraction of the untreated pyrene, the samples were centrifuged at 6000 rpm for 10 min, and the supernatant was separated from the soils and filtered using a syringe filter equipped with a 220 nm membrane filter. The amount of pyrene in acetonitrile was then determined by HPLC (LC-10AS liquid chromatograph, SIL-10AV UV-vis detector, Shimadzu, Japan). The sample injection volume was 10 μL, the mobile phase was acetonitrile-deionized water in a ratio of 9:1, at a flow rate of 1 mL min^{-1}, and detector wavelength 220 nm.

The pyrene degradation in UV condition was performed at least three times, and the results are presented as average ±standard deviation (SD) and the relative SD (RSD). The 2010 Microsoft Excel software was used for the data analysis with a $P_{value} < 0.05$.

Results and Discussion

Characterization of the PA coated photocatalytic nanocomposites

To investigate the crystalline structure of the prepared nanocomposites, the XRD patterns of TiO_2, ZnO, the PA coated TiO_2 and ZnO NPs were obtained. Figure 1(a) shows the XRD patterns of the TiO_2 and TiO_2-PA samples, in which the TiO_2-PA samples display a PA peak close to 34°. In agreement with the reported results in the literature, the XRD patterns of the TiO_2 NPs show several characteristic peaks of the anatase phase of TiO_2 at 25.2°, 28°, 37°, 48°, and 54°. , The diffraction peaks belong to the TiO_2 and PA can be identified by comparison of the XRD patterns between pure TiO_2 and TiO_2-PA (Fig. 1 a). However, extent of crystallinity in TiO_2-PA nanocomposites due to the PA coating is lower than that in pure TiO_2, leading to the shielding of the TiO_2-PA peaks.

Figure 1(b) represents the X-ray diffraction patterns of ZnO and the PA-ZnO nanocomposites. The XRD pattern analysis shows the peaks at 31.84°, 34.52°, 36.33°, 47.63°, 56.71°, 62.96°, 68.13°, and 69.18°, indexed as hexagonal wurtzite phase of ZnO[22]. The diffraction peaks related to PA can be recognized by comparison of XRD patterns of pure ZnO and ZnO-PA.

SEM micrographs can produce very high-resolution images of the sample surface, revealing

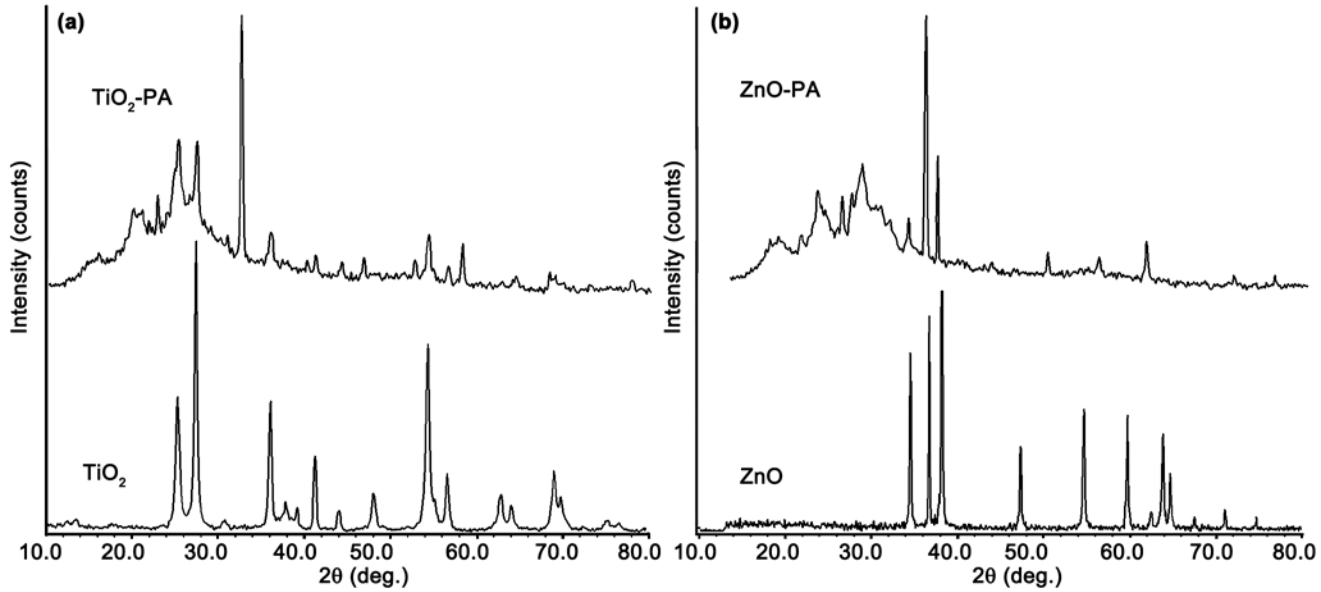

Fig. 1 – X-ray diffraction of (a) TiO_2, TiO_2-PA and (b) ZnO, ZnO-PA photocatalysts.

details of the particle size distribution. According to the SEM images and the SPSS analysis, the TiO_2 and ZnO nanocomposites with 4% PA formed consolidated particles with the size distribution in the range of 100–400 nm, with a high percentage around 200 nm in diameter (Fig. 2). The mean and standard deviation of the particle size distribution calculated by the SPSS analysis are 200.2±71.76 and 159.46±67.16 nm for ZnO–PA 4% and TiO_2–PA 4% NPs, respectively. The nanometric size range of the nanocomposites may be responsible for the catalytic degradation of the pollutants due to their high specific surface area.

FTIR spectroscopy can provide valuable evidence of the PA coating on the nanocomposites. The FTIR spectra of ZnO-PA NPs recorded in the region 4000-400 cm^{-1} shows the characteristic absorption bands of PA at 1575 cm^{-1} (C=N stretching of quinoid ring), 1040.26 $cm^{-1}$and 1302.53 $cm^{-1}$and 1503.09 cm^{-1} (C–N stretching of benzenoid ring), 515.71 cm^{-1} (C–N–C bonding mode of aromatic ring), 592.85 cm^{-1} and 700.84 cm^{-1} (C–C, C–H bonding mode of aromatic ring), 831.98 cm^{-1} (C–H out-of-plane bonding in benzenoid ring)[24]. The FTIR spectra of ZnO and TiO_2 nanoparticles are shown in Fig. S1 (Supplementary Data). The absorption peaks in the range of 400-700 cm^{-1} may be attributed to the Zn-O stretching modes[25].

Furthermore, in ZnO-PA nanocomposites, a broad peak appeared in 3470 cm^{-1} which can be associated to the formation of hydrogen bonding between oxygen of ZnO and H–N group of PA on the surface of the ZnO NPs, which influences the electron densities and bond energies of the PA. Absorption intensity of the ZnO NPs peaks is increased by adding PA to nanocomposites, due to uniform distribution of PA on nanocomposites serface and elimination of agglomeration[26, 27].

However, some of the PA peaks overlap with the ZnO spectra due to the presence of the ZnO in the ZnO-PA NPs (Fig. S1). The FTIR spectra of TiO_2 and TiO_2-PA showed the PA coating on the surface of the TiO_2 NPs. In the FTIR spectrum of TiO_2, a broad peak appeared in the range of 400–700 cm^{-1} due to the vibration of Ti–O–Ti bonds in TiO_2 lattice. FTIR spectrum of TiO_2-PA showed peaks similar to that of TiO_2 NPs associated with the stretching vibration of OH group (3443 cm^{-1}), bending modes of water Ti–OH (1639 cm^{-1}) and vibration of Ti–O–Ti bonds in the range of 400 and 800 cm^{-1}.

The zeta potential measurements yielded the values of 19.5 and 21.2 mV for the TiO_2-PA and ZnO-PA nanocomposites, respectively, which indicates a stable suspension for such a high zeta potential. The positive charge of the NPs is due to the PA coating on the photocatalyst surfaces. When the potential of the two components are opposite, they can combine very well due the electrostatic interaction. TiO_2 and aniline monomer have opposite potential, which is useful for the formation of TiO_2/polyaniline nanocomposite. Hence, TiO_2/polyaniline nanocomposite structure can be formed via electrostatic interaction and may have

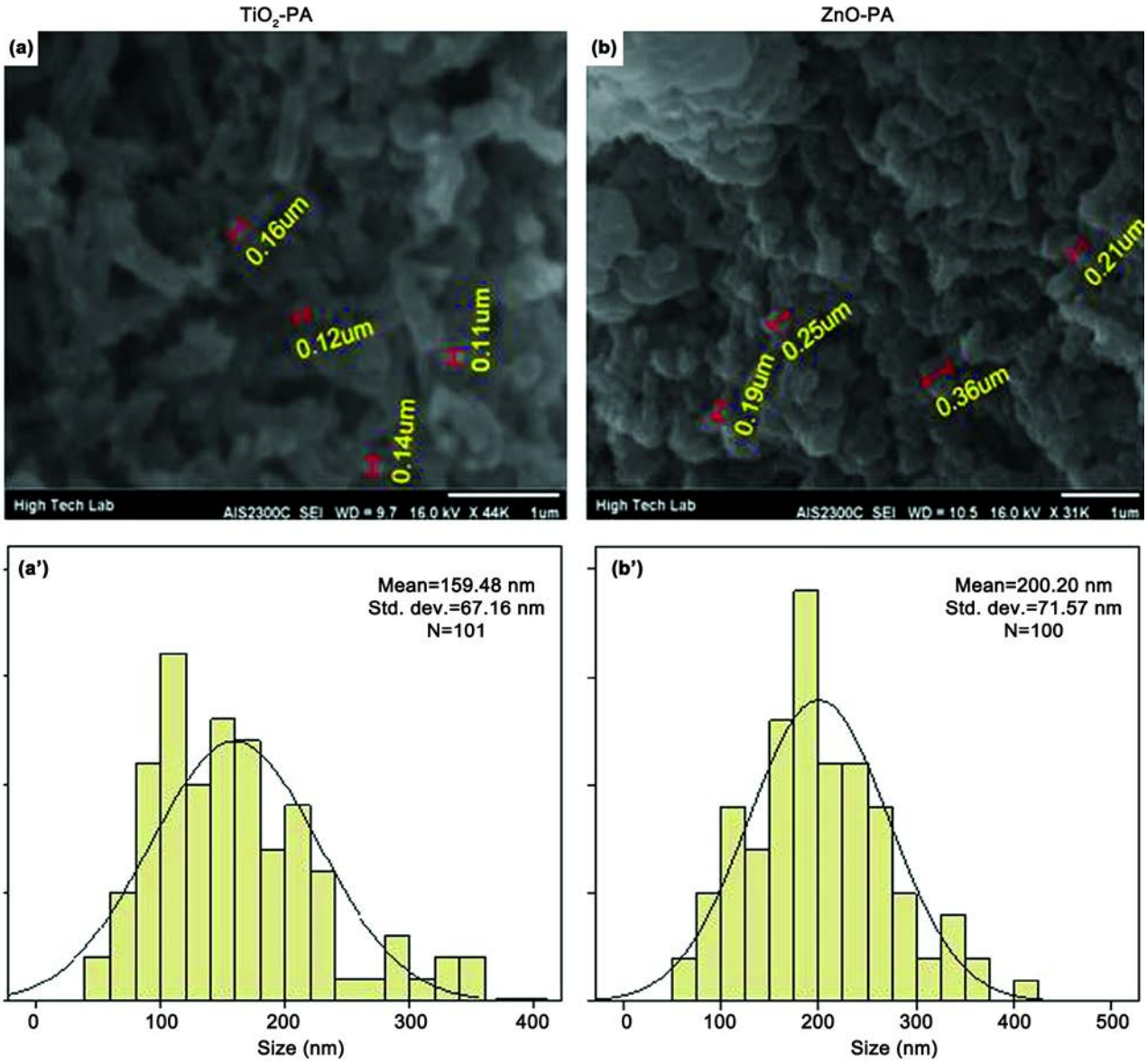

Fig. 2 – SEM micrographs and SPSS analysis of (a, a′) TiO_2-PA4%, and, (b, b′) ZnO-PA4% NPs.

good stability. The surface of nanoparticles can be modified with monolayer dispersed positively charged PA by a facile chemisorption approach[28].

Pyrene degradation

The PAHs removal from the environment has been an important goal of scientists working in the field of treatment of waste water and contaminated soil, and air. The present study discusses the application of newly described PA coated photocatalysts for soil treatment. Figure 3 schematically shows the structure and mode of application of the fabricated photocatalysts mentioned in the study. As

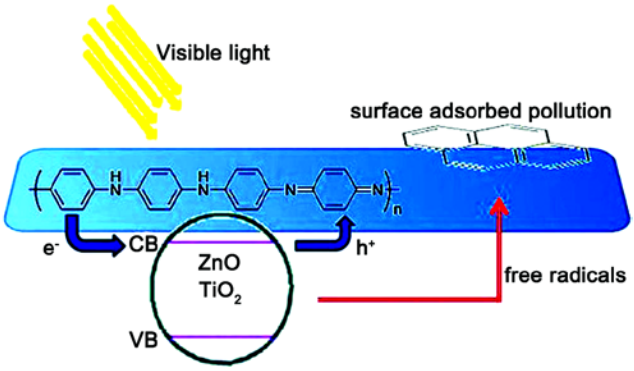

Fig. 3 – The schematic view of the PA coated photocatalysts for the pyrene degradation.

demonstrated in the figure, the semiconductor polymer helps the absorption of the pollutant, improves the transportion of the free radicals, and increases the efficiency of pyrene degradation.

Since PA is a hole acceptor, the oxidative route would be additionally promoted, especially if the homogenous PA is formed on the TiO_2/ZnO surfaces. PA improves the photocatalyst process by enabling the PA-TiO_2 and PA-ZnO synergetic effect, which decreases the h_{VB}^+ and e_{CB}^- recombination process in TiO_2 and ZnO[29].

The HPLC spectrum of pyrene, before and after the treatment with TiO_2–PA photocatalyst is shown in Fig. S2 (Supplementary Data). In the control experiment, a single peak of pyrene was eluted at the retention time of 6 min. The peak area of pyrene was decreased continuously after treatment with the photocatalyst and other small molecules were eluted.

The concentration of pyrene was calculated by comparison of peak area of the sample chromatogram with the peak area of the standard chromatogram[30],

$$\text{Conc. pyrene in sample (mg/L)} = (A_{PYRENE}/A_{STD})\times C_{STD}$$

where A_{PYRENE} is the peak area of sample, A_{STD} is the peak area of standard pyrene compound, and C_{STD} is the concentration of standard pyrene (mg/L).

Effects of the PA addition and reaction time on the catalytic pyrene degradation

Figures 4 and 5 show the effects of ZnO, TiO_2, and the PA modified photocatalysts on the pyrene degradation under UV condition for different dosage samples of the catalyst (0.025, 0.0375, 0.05, and 0.1 g) and at varying reaction times for both the soil samples (P_{value} < 0.05). As shown in Fig. 4, the photocatalysts without the PA coating had a low effect on pyrene degradation under the experimental condition. The PA modified photocatalysts had a positive influence on the pollutant degradation (Fig. 5). However an increase of over 5% *w/w* did not have a significant effect on the pyrene degradation. As shown in Fig. 5 a and c, the pyrene degradation in the bentonite soil sample is higher than that in clay soil sample under the same condition. This may be due to the granular and porous form of bentonite soil.

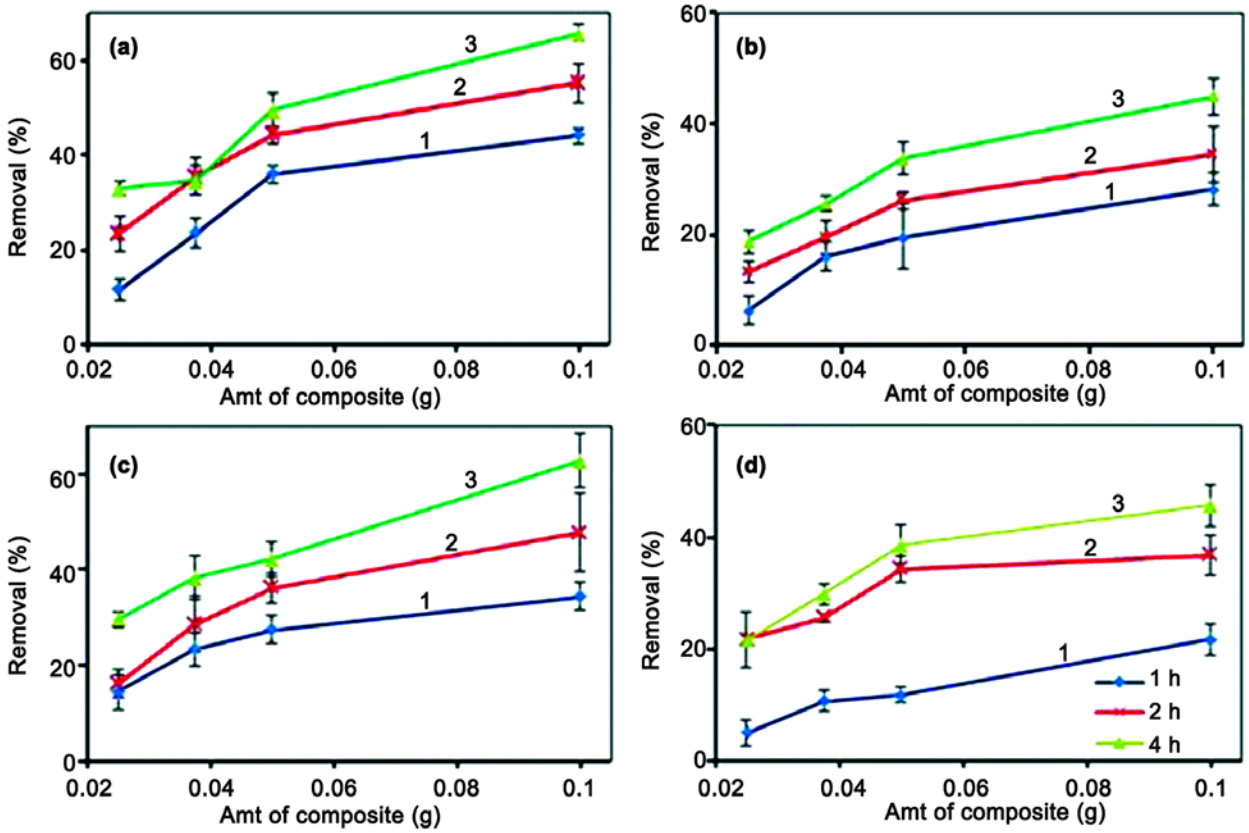

Fig. 4 – Effect of TiO_2 and ZnO on the degradation of the pyrene. [(a) TiO_2 on bentonite sand; (b) TiO_2 on clay; (c) ZnO on bentonite sand; (d) ZnO on clay. 1, 1 h; 2, 2 h; 3, 4 h. Mean of three experiments ±SD; RSD > 10%.].

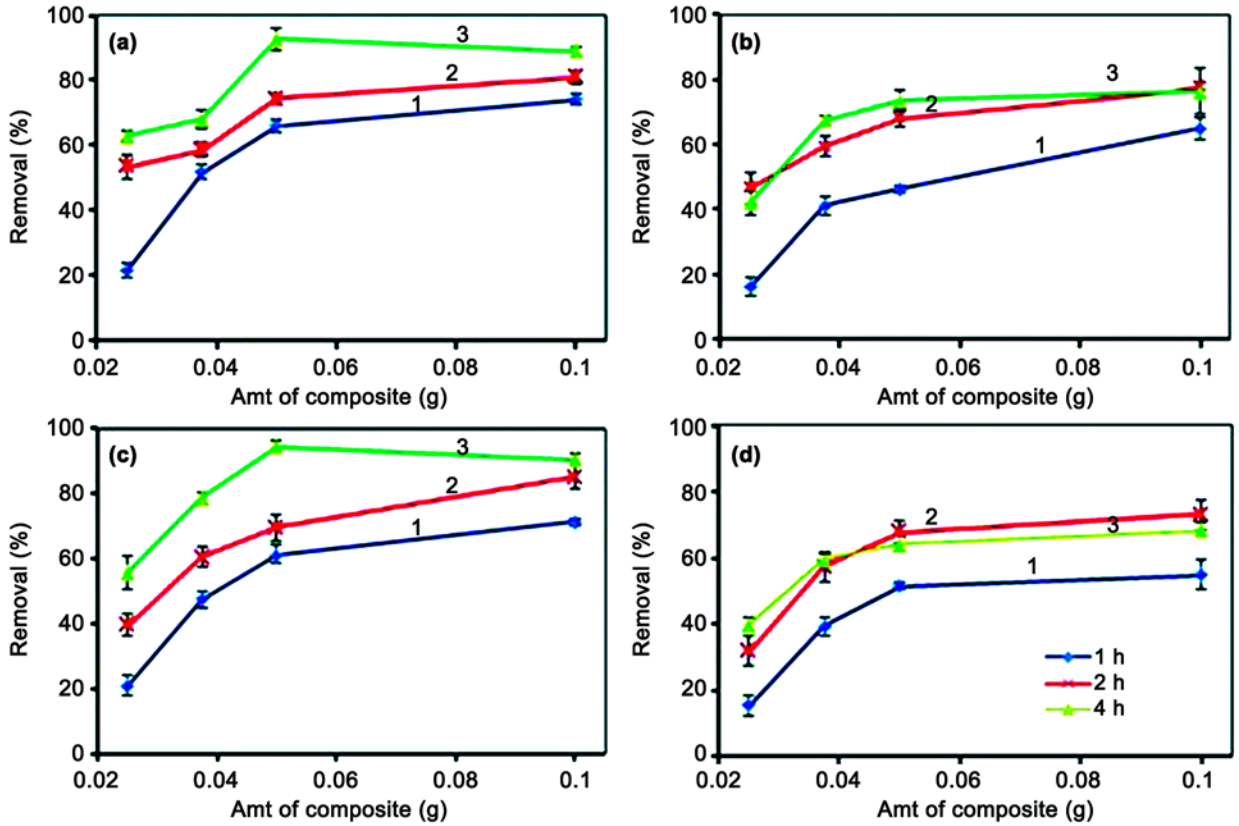

Fig. 5 – Effect of TiO_2-PA(4%) and ZnO-PA(4%) on the degradation of the pyrene. [(a) TiO_2-PA(4%) on bentonite sand; (b) TiO_2-PA(4%) on clay, (c) ZnO-PA(4%) on bentonite sand; (d) ZnO-PA(4%) on clay. 1, 1 h; 2, 2 h; 3, 4 h. Average of three experiments ±SD, RSD < 10% except for amt of composite = 0.025 g for 1 and 2 h].

Treatment under visible irradiation is one of the important aspects of pollutant degradation with photocatalysts. Figure 6 shows the effect of sunlight irradiation on pyrene removal under optimum conditions, which was obtained in the UV condition. As demonstrated, the as-prepared modified photocatalyst degraded the pyrene significantly in this condition. The PA coated photocatalysts, improved the extent of pyrene removal, which was more than 95% for both the ZnO and TiO_2 nanocomposites in the bentonite samples within the visible light condition. This value was lower than 80% for the clay soil under UV radiation, which increased to 90% under sunlight. However, only a maximum degradation of 60% was obtained for the photocatalysts without the polymer. (Fig. 4).

Photocatalytic degradation of pyrene

The polymer doping on the surface of the nanomaterial results in partial oxidation or reduction of the polymer and leads to the formation of positive or negative charges on the surface. The PA doping on

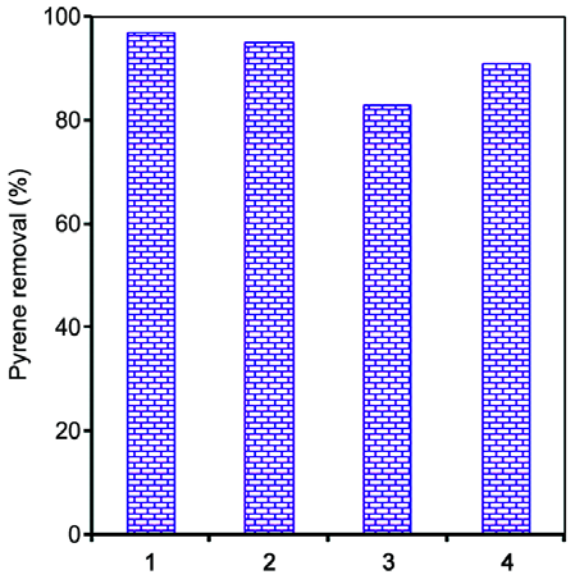

Fig. 6 – Effect of ZnO-PA and TiO_2-PA photocatalysts on the degradation of the pyrene under sunlight irradiation. [1, TiO_2-PA(4%) (bentonite sand); 2, ZnO-PA(4%) (bentonite sand); 3, TiO_2-PA(4%) (clay); 4, ZnO-PA(4%)(clay)].

the photocatalysts leads to (i) high conductivity and photocatalytic activity, (ii) an increase in the concentration of NPs, and (iii) the conjugational defect of the polymer chain, which improves the adsorption capacity of the pollutants[16]. The conductivity of PA, 100 S cm^{-1}, is of the semiconductor level and many orders of magnitude higher than that of common polymers but lower than that of the typical metals [31].

TiO_2 and ZnO can absorb ultraviolet radiation of $\lambda \leq 413$ nm, which induces the valence band electrons (VB) into the conduction band (CB), leaving positive holes (h^+) in the valence band. The possible reaction pathways are given below[32-34]:

$$TiO_2/ZnO + hv \rightarrow TiO_2/ZnO\ (e^-_{CB} + h^+_{VB}) \quad \ldots(1)$$

$$h^+_{VB} + H_2O \rightarrow {}^{\bullet}OH + H^+ \quad \ldots(2)$$

$$e^-_{CB} + O_2 \rightarrow O_2^{\bullet -} \quad \ldots(3)$$

$$O_2^{\bullet -} + H^+ \rightarrow {}^{\bullet}OOH \quad \ldots(4)$$

Equations 1-4 represent a series of reactions using semiconductors.

The holes and free radicals have strong oxidation activity, and can oxidize and even degrade a variety of persistent organic pollutants in the environment. The free radicals play a key role in the photocatalytic oxidation reactions in aqueous suspensions. Also, the electron-hole pairs can directly react with the organic substrates on the surface of the photocatalyst[6, 35]. However, a large band gap of photocatalysts requires UV-vis light for activation. Also, the high degree of recombination between the photogenerated charge carriers, limits their overall photocatalytic efficiency. PA helps to minimize these problems, as the prepared PA-doped photocatalysts are active in visible light. PA can act as an electron source in Eq. 3, thereby acting as oxidizing agent and improving the treatment efficiency.

The polycyclic or larger hydrocarbons strongly absorb UV-vis radiation at wavelengths longer than 300 nm (close to the 350 nm), which exists in sunlight on the earth's surface and are readily photo-oxidized[36]. The oxidation of pyrene may proceed by one-electron transfer, leading to the creation of the pyrene radical. In this study, the pyrene degradation efficiency was increased by the modification of the nanocomposite surface by PA as visible light active photocatalysts. Several studies on efforts to increase the adsorption of the organic pollutants are reported[29, 34, 37]. The present study shows that a good alternative to solve this problem is to incorporate the PA aromatic backbone in the nanocomposite.

It has been reported in literature that degradation of pyrene yields products which are also pollutants[37, 38]. Sigman and his coworkers[39], have reported that pyrene oxidation in water leads to the formation of 1,6- and 1,8-pyrenequinone as stable products. Since the photocatalytic performances of TiO_2 and ZnO were improved by modification with PA, it can be assumed that the PA on the composite surface protected the TiO_2/ZnO surfaces from blocking of the active sites by the intermediates.

PA absorbs visible light to induce π-π* transition under visible radiation. The *d*-orbital (conduction band) of TiO_2/ZnO and the π*-orbital of PA are of similar in energy levels. As a result the excited state electrons of PA are transferred to the *d*-orbital of TiO_2/ZnO, and are subsequently transferred to the surface to react with water and oxygen to yield hydroxyl and superoxide radicals, which would oxidize or degrade the pyrene molecules[40]. Also, in this work thePA-modified TiO_2 and ZnO NPs generated ˙OH when absorbing the sunlight irradiation, which has a suitable energy and other benefits for the degradation of the pyrene in polluted soils [36]. The production of •OH by the absorption of wavelength of sunlight by the PA modified TiO_2 or ZnO leads to the high efficiency of pyrene degradation[41, 42]. Likewise, PA coating increases the surface absorption of organic pollutants and the efficiency of the approach. The obtained photocatalysts can be used for the industrial application of treatment of contaminated soil due to their high stability.

Conclusions

The use of a photocatalyst that is active under sunlight, is one of the cost-effective methods for the removal of pollutants from contaminated soil. In this study, an interfacial polymerization method was used to prepare ZnO-PA and TiO_2-PA nanocomposites. The SEM images confirmed the particle size distribution ~200 nm in diameter. In both XRD and FTIR data, the peaks relating to PA were identified in the nanocomposites. For the extraction of pyrene of the soil samples, a continuous batch extraction was carried out and evaluated. The data analysis showed the positive effect of PA on pyrene degradation under UV and sunlight radiation, by decreasing the electron-hole recombination in modified photocatalysts. The

PA coated photocatalysts, improved the extent of pyrene removal, which was more than 95% for both the ZnO and TiO_2 nanocomposites in the bentonite samples under the visible light condition. This value was lower than 80% for the clay soil under UV radiation, which increased to 90% under sunlight. However, only a maximum degradation of 60% was obtained with the unmodified photocatalysts. The increase in the degradation efficiency was due to the increase in adsorption of the organic molecules from the bentonite and clay soils by polyaniline, and also the semiconducting behavior of polymer, that prevented the electron-hole recombination, causing an increase in the photocatalytic activity under both UV and visible radiation. The new ZnO/PA and TiO_2/PA photocatalysts are believed to be promising photocatalytic materials, which can be widely used for the treatment of environmental pollution.

Supplementary Data

Supplementary data associated with this article are available in the electronic form at http://www.niscair.res.in/jinfo/ijca/IJCA_57A(05)610-618_SupplData.pdf.

Acknowledgment

This work has been fully supported by Iran National Science Foundation (INSF) under the project 90003443.

References

1 Ravindra K, Sokhi R & Van Grieken R, *Atmos Environ*, 42 (2008) 2895.
2 Xia X, Li G, Yang Z, Chen, Y & Huang G H, *Environ Pollut*, 157 (2009), 1352.
3 Wohak L E, Krais A M, Kucab J E, Stertmann J, Øvrebø S, Seidel A, Phillips D H & Arlt V M, *Arch Toxicol*, 90 (2016) 291.
4 Panda N, Sahoo H & Mohapatra S, *J Hazard Mater*, 185 (2011) 359.
5 Zeng Y, Hong P A & Wavrek D A, *Environ Sci Technol*, 34 (2000) 854.
6 Chien S C, Chang C, Chen S, Wang M, Rao M M & Veni S S, *Sci Total Environ*, 409 (2011) 4101.
7 Jan S, Kamili A N, Parween T, Hamid R, Parray J A, Siddiqi T, Mahmooduzzafar & Parvaiz A, *Desalin Water Treat*, 55 (2015) 2053.
8 Masoudian S, Rasoulifard M H & Pakravan P, *Indian J Chem*, 54A (2015) 757.
9 Shahadat M, Nabi S, Bushra R, Raeissi A, Umar K & Ansari M O, *RSC Adv*, 2 (2012) 7207.
10 Gnanaprakasam A, Sivakumar V M, Sivayogavalli P L & Thirumarimurugan M, *Ecotoxicol Environ Saf*, 121 (2015) 121.
11 Mansouri A, Shahrezaei F, Zinatizadeh A, Azandaryani A H, Pirsaheb M & Sharafi K, *J Taiwan Inst Chem E*, 45 (2014) 2501.
12 Shahrezaei F, Pakravan P, Azandaryani A H, Pirsaheb M & Mansouri A, *Desalin Water Treat*, 57 (2016) 14443.
13 Khan R, Shamshi Hassan M., Uthirakumar P, Yun J H, Khil M S & Lee I H, *Mater Lett*, 152 (2015) 163.
14 Shahrezaei F, Mansouri Y, Zinatizadeh A A L & Akhbari A, *Powder Technol*, 221 (2012) 203.
15 Qin W, Zhu Y, Fan F, Wang Y, Liu X, Ding A & Dou J, *Biochem Eng J*, 121 (2017) 131.
16 Ameen S, Shin H S, Akhtar M S & Kim Y S, *Fabrication, Doping and Characterization of Polyaniline and Metal Oxides: Dye Sensitized Solar Cells*, edited by L Kosyachenko, (Intech Open Access Publisher, UK) 2011.
17 Deng F, Zhang Z, Yang C, Guo C, Lu G & Dang Z, *Ecotoxicol Environ Saf*, 138 (2017) 9.
18 Zhao X, Ma K, Jiao T, Xing R, Ma X, Hu J, Huang H, Zhang L & Yan X, *Sci Rep*, 7 (2017) 44076.
19 Zarrini K, Rahimi A A, Alihosseini F & Fashandi H, *J Clean Prod*, 142 (2017) 3645.
20 Huang J, Virji S, Weiller B H & Kaner R B, *J Am Chem Soc*, 125 (2003) 314.
21 *MIP_4 (ver. 1.0)*, (Nahamin Pardazan Asia Co., Iran); www.metsofts.ir.
22 Dong D, Li P, Li X, Xu C, Gong D, Zhang Y, Zhao Q & Li P, *Chem Eng J*, 158 (2010) 378.
23 Talam S, Karumuri S R & Gunnam N, *ISRN Nanotechnol*, 2012 (2012); doi:10.5402/2012/372505.
24 Taleghani H, Aleahmad M & Eisazadeh H, *World Appl Sci J*, 6 (2009) 1607.
25 Sharma N, Jandaik S, Kumar S, Chitkara M & Sandhu I S, *J Exper Nanosci*, 11 (2016) 54.
26 Mostafaei A & Zolriasatein A, *Prog Nat Sci: Mater Int*, 22 (2012) 273.
27 Chakraborti S, Joshi P, Chakravarty D, Shanker V, Ansari Z, Singh S P & Chakrabarti P, *Langmuir*, 28 (2012) 11142.
28 Tian X, He K, Wang C, Wen Q, Wang B, Yu S, Hao C, Chen K & Lei Q, *Compos Sci Technol*, 137 (2016) 118.
29 Gilja V, Novaković K, Travas-Sejdic J, Hrnjak-Murgić Z, Roković M K & Žic M, *Nanomater*, 7 (2017) 412.
30 Agrawal N, Verma P & Shahi S K, *Bioresource Bioprocess*, 5 (2018) 11.
31 Stejskal J & Gilbert R, *Pure Appl Chem*, 74 (2002) 857.
32 Grabowska E, Reszczyńska J & Zaleska A, *Water Res*, 46 (2012) 5453.
33 Gholami M, Nassehinia H R, Jonidi-Jafari A, Nasseri S & Esrafili A, *J Environ Health Sci Eng*, 12 (2014) 45.
34 Mondal K, Bhattacharyya S & Sharma A, *Indus Eng Chem Res*, 53 (2014) 18900.
35 Wen S, Zhao J, Sheng G, Fu J & Peng P, *Chemosphere*, 50 (2003) 111.
36 Srikant V & Clarke D R, *J Appl Phys*, 83 (1998) 5447.
37 Oliveira A S, Ferreira L, Da Silva J & Moreira J C, *Int J Photoenergy*, 6 (2004) 205.
38 Zhu F, Storey S, Ashaari M M, Clipson N & Doyle E, *Environ Sci Pollut Res*, 24 (2017) 5404.
39 Sigman M E, Schuler P F, Ghosh M M & Dabestani R, *Environ sci technol*, 32 (1998) 3980.
40 Sandhya K, Haridas S & Sugunan S, *Bull Chem React Eng Catal*, 8 (2013) 145.
41 Hoffmann M R, Martin S T, Choi W & Bahnemann D W, *Chem rev*, 95 (1995) 69.
42 Malato S, Blanco J, Vidal A & Richter C, *Appl Catal Environ*, 37 (2002) 1.